

# UCSF

## UC San Francisco Previously Published Works

### Title

Evaluation of a Novel Macromolecular Cascade-Polymer Contrast Medium for Dynamic Contrast-Enhanced MRI Monitoring of Antiangiogenic Bevacizumab Therapy in a Human Melanoma Model

### Permalink

<https://escholarship.org/uc/item/75z9z5wb>

### Journal

Academic Radiology, 20(10)

### ISSN

1076-6332

### Authors

Cyran, Clemens C  
Fu, Yanjun  
Rogut, Victor  
et al.

### Publication Date

2013-10-01

### DOI

10.1016/j.acra.2013.07.010

Peer reviewed

Published in final edited form as:

Acad Radiol. 2013 October ; 20(10): . doi:10.1016/j.acra.2013.07.010.

## Evaluation of a Novel Macromolecular Cascade-Polymer Contrast Medium for Dynamic Contrast-Enhanced MRI Monitoring of Antiangiogenic Bevacizumab Therapy in a Human Melanoma Model

Clemens C. Cyran, MD, Yanjun Fu, PhD, Victor Rogut, MD, Bundit Chaopathomkul, MD, Michael F. Wendland, PhD, David M. Shames, MD, and Robert C. Brasch, MD

Center for Pharmaceutical and Molecular Imaging, Department of Radiology, University of California San Francisco, San Francisco, California (C.C.C., Y.F., V.R. B.C., M.F.W., D.M.S., R.C.B.); and Department of Clinical Radiology, Laboratory for Experimental Radiology, University Hospitals Munich, Campus Grosshadern, Marchioninistrasse 15, 81377 Munich, Germany (C.C.C.)

### Abstract

**Rationale and Objectives**—To assess the applicability of a novel macromolecular polyethylene glycol (PEG)-core gadolinium contrast agent for monitoring early antiangiogenic effects of bevacizumab using dynamic contrast-enhanced (DCE) magnetic resonance imaging (MRI).

**Materials and Methods**—Athymic rats ( $n = 26$ ) implanted with subcutaneous human melanoma xenografts underwent DCE-MRI at 2.0 T using two different macromolecular contrast agents. The PEG core cascade polymer PEG12,000-Gen4-(Gd-DOTA)<sub>16</sub>, designed for clinical development, was compared to the prototype, animal-only, macromolecular contrast medium (MMCM) albumin-(Gd-DTPA)<sub>35</sub>. The treatment ( $n = 13$ ) and control ( $n = 13$ ) group was imaged at baseline and 24 hours after a single dose of bevacizumab (1 mg) or saline to quantitatively assess the endothelial-surface permeability constant ( $K^{PS}$ ,  $\mu\text{L}\cdot\text{min}\cdot 100\text{ cm}^3$ ) and the fractional plasma volume (fPV, %), using a two-compartment kinetic model.

**Results**—Mean  $K^{PS}$  values, assessed with PEG12,000-Gen4-(Gd-DOTA)<sub>16</sub>, declined significantly ( $P < .05$ ) from  $29.5 \pm 10\ \mu\text{L}\cdot\text{min}\cdot 100\text{ cm}^3$  to  $10.4 \pm 7.8\ \mu\text{L}\cdot\text{min}\cdot 100\text{ cm}^3$  by 24 hours after a single dose of bevacizumab. In parallel,  $K^{PS}$  values quantified using the prototype MMCM albumin-(Gd-DTPA)<sub>35</sub> showed an analogous, significant decline ( $P < .05$ ) in the therapy group. No significant effects were detected on tumor vascularity or on microcirculatory parameters in the control group between the baseline and the follow-up scan at 24 hours.

**Conclusion**—DCE-MRI enhanced with the novel MMCM PEG12,000-Gen4-(Gd-DOTA)<sub>16</sub> was able to monitor the effects of bevacizumab on melanoma xenografts within 24 hours of a single application, validated by the prototype, animal-only albumin-(Gd-DTPA)<sub>35</sub>. PEG12,000-Gen4-(Gd-DOTA)<sub>16</sub> may be a promising candidate for further clinical development as a macromolecular blood pool contrast MRI agent.

## Keywords

Dynamic MRI; gadolinium polyethylene glycol polymer contrast agent; human melanoma xenograft; bevacizumab; anti-angiogenesis effect

Functional and molecular imaging techniques have been examined extensively to define their potential for monitoring the tumor angiogenesis. Established morphologic assessments relying on tumor size such as Response Evaluation Criteria in Solid Tumors (RECIST) 1.1 do not have adequate sensitivity for detection of tumor responses to antiangiogenic therapy in a desirable short time period (1). Data indicate that magnetic resonance (MR) morphology alone, including size or contrast enhancement, will not be adequate to monitor angiogenesis treatment (2). Dynamic, contrast-enhanced (DCE) MR imaging (MRI) enhanced with macromolecular contrast media (MMCM) has been investigated in experimental studies for monitoring tumor angiogenesis, based on the dependence of endothelial macromolecular permeability on tissue vascular endothelial growth factor (VEGF) activity. VEGF potentially increases macromolecular permeability whereas inhibition of VEGF, shown with a variety of antiangiogenesis drugs and cancer models, reduces macromolecular permeability (3–6). The range of diagnostic utility for MMCM-enhanced MRI in cancer characterization has been demonstrated in recent years using animal models and the prototypic MMCM albumin-(Gd-DTPA)<sub>35</sub> in differentiating benign and malignant tumors, in grading the degree of tumor aggressiveness, in detecting early responses to antiangiogenesis drug therapy, and in use as a predictive biomarker of tumor response (3,7–9). However, albumin-(Gd-DTPA)<sub>35</sub> is considered to be poorly suited for use in humans because of incomplete elimination and concerns of immunogenicity (10). Hence, new MMCM are being sought that have blood kinetic properties similar to albumin-(Gd-DTPA)<sub>35</sub> and will be appropriate for application in humans. Among currently investigated macromolecular contrast agents are polymers, dendrimers, and noncovalent complexes of small molecule agents with proteins including novel biodegradable compounds such as a polydisulfide with Gd-DOTA monoamide side chains (11) or triazine dendrimers derivatized with a DOTA or DTPA (12).

The current study advances the evaluation of polyethylene glycol (PEG) core Gd macromolecular contrast agents, specifically PEG12,000-Gen4-(Gd-DOTA)<sub>16</sub>, representing a novel class of macromolecular contrast agents. PEG-core MMCM are designed specifically for clinical safety in humans, while meeting the physicochemical and pharmacologic requirements of contrast agents intended for quantitative MRI characterization of blood vessels (13–15). This initial experimental study was conducted to investigate the applicability of PEG12,000-Gen4-(Gd-DOTA)<sub>16</sub> for monitoring of antiangiogenic therapy analogous to the established prototype albumin-(Gd-DTPA)<sub>35</sub>.

Bevacizumab is a humanized monoclonal antibody directed against VEGF-A, a potent signaling molecule produced by many types of cancer cells. VEGF promotes angiogenesis known to result in new tumor vessel formation necessary for both exponential growth and metastasis. Bevacizumab was the first governmentally approved and commercially available angiogenesis inhibitor in the United States and it remains in approved clinical use for treatment of colon, lung, kidney, and brain cancers (16). The Food and Drug Administration decision to revoke bevacizumab approval in breast cancer patients in November 2011 was mainly based on the circumstance that patients risk potentially life-threatening side effects without definite proof that bevacizumab will provide a benefit, such as delay tumor growth, that would justify those risks (17). This underscores the need in health care to identify clinically feasible, quantitative, cost-effective, and reliable methods to characterize tumor on an individual patient basis (18). An imaging-based technique capable of monitoring angiogenesis inhibition on an individual patient basis could find widespread application in

the management of patients with breast cancer or other neoplastic diseases. The technique ideally should indicate efficacy of therapy both quickly and, in the case of drugs, after only a single test administration.

We therefore hypothesized that DCE-MRI enhanced with the novel PEG-core MMCM is able to assess the early antiangiogenic effects of bevacizumab on experimental melanoma xenografts 24 hours after a single dose, compared to an established, animal-only prototype MMCM, albumin-(Gd-DTPA)<sub>35</sub>. The purpose of our study was to investigate if significant changes in tumor endothelial permeability or tumor vascularity induced by bevacizumab can be assessed with PEG12,000-Gen4-(Gd-DOTA)<sub>16</sub> and compare the results to albumin-(Gd-DTPA)<sub>35</sub> for validation purposes.

## Materials and Methods

### Animal Model

Experiments were conducted in accordance with guidelines for the care and use of laboratory animals as described by the National Institutes of Health and were approved by the institutional animal care committee. A total of 26 athymic rats (Hsd: RH-Foxn1<sup>tmu</sup>, Harlan, Indianapolis, Indiana) were implanted with subcutaneous melanoma xenografts (MDA-MB-435) over the right abdominal flank, randomized to the therapy ( $n = 13$ ) or the control group ( $n = 13$ ), and imaged by DCE-MRI at 2.0 T. In the treatment and control group, seven subjects were investigated by PEG12,000-Gen4-(Gd-DOTA)<sub>16</sub>-enhanced MRI; in six subjects, MRI was enhanced with albumin-(Gd-DTPA)<sub>35</sub>. All rats were imaged twice, at baseline and 24 hours after a single intraperitoneal dose of bevacizumab (1 mg) or a volume-equivalent injection of saline. DCE-MRI enhancement data were analyzed using a two-compartment kinetic model, described in detail elsewhere (19), to generate quantitative estimates of the endothelial-surface permeability constant ( $K^{PS}$ ) ( $\mu\text{L}\cdot\text{min}^{-1}\cdot 100\text{ cm}^3$ ) as a parameter of vascular permeability, and the fractional plasma volume (fPV, %) as a parameter of tumor vascularity.

### Contrast Media

Seven bevacizumab-treated and seven control subjects received the PEG-cascade polymer PEG12,000-Gen4-(Gd-DOTA)<sub>16</sub> (Fig 1) with an effective molecular weight of 194 kDa and a T1-relaxivity ( $\text{mM}^{-1}\text{s}^{-1}$ ) of 9.9 (at 10 MHz and 37°C) (13–15,20) by standardized fast manual bolus injection via a tail vein catheter at a dose of 0.04 mmol Gd/kg body weight. The remaining 12 subjects were imaged using the prototype MMCM albumin-(Gd-DTPA)<sub>35</sub>, synthesized in our laboratory following the methods of Ogan et al (21). This prototype MMCM has an effective molecular weight of a 180 kDa, a T1-relaxivity of 11  $\text{mM}^{-1}\text{s}^{-1}/\text{Gd}$  ion and 385  $\text{mM}^{-1}\text{s}^{-1}/\text{Gd}$  albumin core, was administered at a dose of 0.03 mmol Gd/kg body weight. Blood half-lives for PEG12,000-Gen4-(Gd-DOTA)<sub>16</sub> and for albumin-(Gd-DTPA)<sub>35</sub> were 49 ± 6 minutes and 54 ± 11 minutes, respectively (14).

### PEG Core MMCM Synthesis

PEG diols (the form of PEG with two hydroxyl terminal groups) having near-uniform size (polydispersity index < 1.05) and molecular weights of 12,000 Da were used as starting materials (Nektar Therapeutics, Huntsville, Alabama). The PEG diols were converted to the bisamine, followed by a multistep divergent dendrimer synthesis based on the PEG bisamine conducted using N2, N6-di-t-butyloxycarbonyl (Boc) L-lysine as the repeating unit via t-Boc peptide chemistry. Specifically, four cycles (eight steps) were needed for the synthesis of generation-4 dendrimers. PEG12,000-Gen4-(Gd-DOTA)<sub>16</sub> has 32 amino groups, in theory, available for conjugation. For these synthesized polymeric amines, the difference between the measured and theoretical number of amino groups was found to be <5%.

Polymeric amines were then conjugated in *N,N*-dimethylformamide with the monofunctionalized, amino-reactive, succinimidyl ester of tri-*t*-butyl DOTA-MeGly, synthesized from its carboxy precursor. The resulting polymer-DOTA conjugates were then treated with 1:1 trifluoroacetic acid/water to remove the protecting *t*-butyl groups, and then complexed with Gd ions at pH 5. After further purification by dialysis the PEG-core dendrimeric contrast agent PEG12,000-Gen4-(Gd-DOTA)<sub>16</sub> was obtained. The purity of the final MMCM product was confirmed by size-exclusion HPLC (>99.9%) and formulated as a 20 mM Gd solution and sterile-filtered twice.

### Dynamic MRI

For both contrast media, MRI was performed using an Omega CSI-II system operating at 2.0 Tesla (Bruker Instruments, Fremont, California). The system is equipped with Acustar S-150 self-shielded gradient coils. Rats were placed within a custom-built, birdcage radiofrequency coil (length 7.6 cm, inner diameter 4.5 cm) in the supine position. A series of nine precontrast T1-weighted inversion recovery centric-ordered fast gradient-recalled echo images (repetition time/echo time = 6.0/1.5 milliseconds, NA = 1, flip angle  $\alpha = 10^\circ$ , matrix  $64 \times 64$  field of view  $50 \times 50$  mm, slice thickness = 3 mm), with TI varying between 100 and 2500 milliseconds, were obtained to calculate baseline relaxation rates (R1) for tumor in each animal by curve fitting (22). Because the inversion recovery snapshot fast low-angle shot method is inadequate for measuring the R1 of flowing blood, the baseline R1 in the inferior vena cava was taken to be  $0.752 \text{ seconds}^{-1}$ , which is the mean blood R1 in rats at  $37^\circ \text{ C}$  and 2 Tesla measured in more than 200 previous specimens (8). Dynamic MRI was performed using a T1-weighted three-dimensional spoiled gradient refocused sequence acquiring two precontrast and 28 postcontrast images with high spatial resolution and repetition time = 50 ms, echo time = 3 ms, NA = 1, flip angle ( $\alpha$ ) =  $90^\circ$ , matrix =  $128 \times 128 \times 16$ , field of view =  $50 \times 50 \times 48$  mm, slice thickness = 3 mm, acquisition time 1 minute, 42 seconds, per image.

### Data Analysis

A Sun Sparc 10 workstation (Sun Microsystems, Mountain View, California) with MR Vision Software (MR Vision Co., Winchester, Massachusetts) was used to process and analyze the acquired image data. Regions of interest signal intensity measurements were acquired over the blood in the inferior vena cava and the tumor periphery at each time point. The tumor periphery was defined as the outer 2-mm rim of the whole tumor, shown in previous studies to be a sensitive tumor zone in which to evaluate the effects of angiogenesis inhibitors on vital tumor tissue (23). Post-contrast R1 values were calculated based on the measured signal intensities and the calculated values of precontrast R1 based on the inversion recovery data. Differences between the precontrast and post-contrast R1 values ( $\Delta R1$ ) in blood as well as in tumor tissue were assumed to be directly proportional to the concentration of gadolinium in the tissue. Estimates of the  $K^{PS}$  ( $\mu\text{L}\cdot\text{min}\cdot 100 \text{ cm}^3$ ) and the fPV (%) were calculated based on kinetic analysis of the  $\Delta R1$  data. Briefly, a monoexponential function was used to fit the blood  $\Delta R1$  data, serving as a forcing function for the two-compartment, unidirectional kinetic model used to fit the tumor  $\Delta R1$  data. Both blood and tissue models were fit to the data concurrently using the SAAM II software (SAAM Institute, Seattle, Washington), which employs a weighted, nonlinear least-squares estimation algorithm. Measurement errors in the  $\Delta R1$  data were assumed to be independent and Gaussian, with zero mean and fractional standard deviation (SD) known within a scale factor determined from the data. Weights were optimally chosen (ie, equal to the inverse of the variance of the measurement error). The precision of the parameter value estimates was determined from the covariance matrix at the least-squares fit. For statistical analysis, comparison of MMCM-based estimates for  $K^{PS}$  and fPV was performed using one-way analysis of variance. Statistical significance was defined as  $P < .05$ . All statistical testing

was performed using the GraphPad *Prism* software (GraphPad software, San Diego, California).

## Results

Contrast agents were well tolerated in all animals without adverse effects noted during the course of the experiment. Mean tumor volume at baseline in the therapy group was  $826 \pm 35$  mm<sup>3</sup>, in the control group  $797 \pm 26$  mm<sup>3</sup>, measured in three dimensions by caliper, with no significant effects on tumor size within the short 24-hour course of the experiment. Individual values for MRI-estimated parameters of tumor microcirculation are presented in Table 1 and Figure 2. Theoretical and measured effective molecular weights (MW), T1 relaxivities, and blood half-lives for PEG12,000-Gen4-(Gd-DOTA)<sub>16</sub> and albumin-(Gd-DTPA)<sub>35</sub> are presented in Table 2.

### DCE-MRI Enhanced With PEG12,000-Gen4-(Gd-DOTA)<sub>16</sub>

In the bevacizumab-treated therapy group imaged with PEG12,000-Gen4-(Gd-DOTA)<sub>16</sub>, the K<sup>PS</sup> declined significantly ( $P < .05$ ) from baseline to 24 hours after a single dose of bevacizumab ( $29.5 \pm 10.4$   $\mu\text{L}\cdot\text{min}\cdot 100$  cm<sup>3</sup> to  $10.4 \pm 7.8$   $\mu\text{L}\cdot\text{min}\cdot 100$  cm<sup>3</sup>). Using the same PEG core MMCM, no significant change in K<sup>PS</sup> was observed in the control group between baseline and 24-hour measurements ( $41 \pm 34$   $\mu\text{L}\cdot\text{min}\cdot 100$  cm<sup>3</sup> vs.  $35 \pm 14$   $\mu\text{L}\cdot\text{min}\cdot 100$  cm<sup>3</sup>). No significant change in tumor vascularity was detected over 24 hours for either the bevacizumab- or the saline-treated tumors (fPV%, bevacizumab group:  $3.1 \pm 1.6\%$  vs.  $3.6 \pm 1.4\%$ ,  $P > .05$ , saline group:  $4.5 \pm 1.3\%$  vs.  $4.2 \pm 1.1\%$ ,  $P > .05$ ). A representative set of PEG-enhanced DCE-MRI images is shown in Figure 3.

### DCE-MRI Enhanced With Albumin-(Gd-DTPA)<sub>35</sub>

DCE-MRI in bevacizumab-treated tumors enhanced with albumin-(Gd-DTPA)<sub>35</sub> revealed a significant reduction ( $P < .05$ ) of K<sup>PS</sup> between baseline and 24 hours ( $32 \pm 15$   $\mu\text{L}\cdot\text{min}\cdot 100$  cm<sup>3</sup> to  $0$   $\mu\text{L}\cdot\text{min}\cdot 100$  cm<sup>3</sup>), in agreement with the declining endothelial permeability in the bevacizumab-treated tumors imaged with PEG12,000-Gen4-(Gd-DOTA)<sub>16</sub>. Of note, in the experiment using albumin-(Gd-DTPA)<sub>35</sub>, endothelial permeability dropped below detection level in all seven investigated tumors (K<sup>PS</sup> at 24 hours =  $0$   $\mu\text{L}\cdot\text{min}\cdot 100$  cm<sup>3</sup>). No significant effects were detected on endothelial permeability in control groups or on tumor vascularity in the therapy or the control group ( $P > .05$ ). A representative set of DCE-MRI images enhanced with albumin-(Gd-DTPA)<sub>35</sub> is shown in Figure 4.

## Discussion

With increasing clinical application of novel molecular cancer therapies, such as inhibitors of angiogenesis, functional and molecular imaging modalities are increasingly complementing established morphological imaging. These techniques, such as RECIST 1.1, have been shown to be not sufficiently sensitive for timely monitoring of therapy (1). However, the use of DCE-MRI does allow for the noninvasive investigation of functional parameters of tissue microcirculation that may be applicable as imaging biomarkers of therapy response to anti-angiogenic therapies (24). Additionally, novel developments in molecular imaging including nanosized contrast agents and theranostic agents increasingly allow for the characterization of the tumor microenvironment on a cellular level with options for dedicated drug delivery (25–27). Published studies on the applicability of DCE-MRI with clinically available small-molecular contrast medium (molecular weight <1 kDa) for monitoring angiogenesis and anti-angiogenic therapies reveal controversial results with regard to the pathophysiologic correlate and validity of the assessed noninvasive parameters of microcirculation (28,29). Additionally, a lack in standardization of acquisition and



postprocessing protocols (30) may be in part responsible that some investigators had difficulties to duplicate each others' results (31). Alternatively, macromolecular contrast media (molecular weight >60 kDa) have been proposed for monitoring antiangiogenic treatment because they follow a primarily intravascular distribution profile with a pronounced extravasation through the hyperpermeable endothelium of angiogenically active tissues under VEGF stimulation, allowing for a sensitive assessment of angiogenic activity in tumors (29,32).

Results of our study show that PEG12,000-Gen4-(Gd-DOTA)<sub>16</sub> and albumin-(Gd-DTPA)<sub>35</sub> perform in similar fashion in the monitoring of antiangiogenic effects of bevacizumab using DCE-MRI. The novel MMCM PEG12,000-Gen4-(Gd-DOTA)<sub>16</sub>, based on a linear backbone of PEG, with an effective MW in the range of circulating proteins, can be applied to assess the therapeutic response to a single dose of the VEGF antibody bevacizumab in human melanoma xenografts in rats using DCE-MRI. A statistically significant ( $P < .05$ ) reduction in  $K^{PS}$  to the macromolecular contrast agent PEG12,000-Gen4-(Gd-DOTA)<sub>16</sub> was detectable only 24 hours after administration of the VEGF-inhibiting drug. Our current results are in line with a published study (14) investigating DCE-MRI enhanced with PEG, gadolinium-based contrast media of different molecular weights, including PEG12,000-Gen4-(Gd-DOTA)<sub>16</sub>, in subcutaneous tumor xenografts and healthy tissues that showed a significantly stronger extravasation of PEG12,000-Gen4-(Gd-DOTA)<sub>16</sub> molecules was present in angiogenically active tumor tissue than in angiogenically less active muscle. This finding may also reflect the significantly reduced extravasation of PEG12,000-Gen4-(Gd-DOTA)<sub>16</sub> molecules in the investigated melanoma xenografts following angiogenesis inhibition with bevacizumab. PEG core MMCM, which contain numerous covalently bound stable, macrocyclic chelates of gadolinium, were designed specifically for clinical safety while retaining physicochemical and pharmacologic properties essential for quantitative MR vascular imaging (15). All the individual components of the assembled PEG-based MMCM including the polymeric PEG core, terminal amino cascade functions, and DOTA chelates of gadolinium are previously shown to be well-tolerated in humans and each single component is currently approved for clinical application (14,15).

Corresponding to the experiments with PEG12,000-Gen4-(Gd-DOTA)<sub>16</sub>, a statistically significant reduction of  $K^{PS}$  was observed using albumin-(Gd-DTPA)<sub>35</sub>. Of interest, each of the seven melanoma xenografts investigated with albumin-(Gd-DTPA)<sub>35</sub> showed a decline of tumor endothelial permeability below the detection level 24 hours after the administration of bevacizumab. The degree of the vascular response varied for both investigated MMCM with the specific tumor with pre- versus post- $K^{PS}$  differences ranging from zero (no change) to 100% declines in response to bevacizumab treatment. This demonstration of a variable but gradable response can be anticipated based on the recognized variability in cancer biology and in drug responsiveness for individual tumors: even cancers with similar histopathology can differ widely in behavior and VEGF expression (32). The specific biology that underlies the application of macromolecular probes to assess the angiogenesis process is that permeability to macromolecular solutes is a direct indication of the activity of VEGF. VEGF is the highly potent signaling molecule that plays a central role in the angiogenesis process. VEGF, also known as vascular permeability factor, increases the in-growth of new cancer microvessels, while simultaneously increasing macromolecular permeability as much as 50,000 times more strongly than histamine (33). Inhibition of VEGF, shown with an array of antiangiogenesis drugs and in multiple cancer types, reduces macromolecular permeability (3–6,14,32). With regard to tumor vascularity, neither PEG12,000-Gen4-(Gd-DOTA)<sub>16</sub> nor albumin-(Gd-DTPA)<sub>35</sub> showed a significant change of fractional plasma volume following bevacizumab treatment in the therapy group or from the administration of saline in the control group.

Unlike the PEG core MMCM design, albumin-(Gd-DTPA)<sub>35</sub> was never intended for human use because of concerns for immune-mediated toxicity and limited stability of the DTPA chelate for gadolinium. The current study extends earlier encouraging results produced with the use of albumin-(Gd-DTPA)<sub>35</sub> by demonstrating the applicability of a class of novel MMCM based on a linear core of PEG with numerous macrocyclic DOTA chelates of gadolinium attached to both ends. The molecular design takes advantage of the known clinical safety and high water solubility of PEG combined with the high thermodynamic stability and demonstrated safety of the DOTA-Gd complex to yield the desired large molecular configuration to mimic the vascular permeability and distribution behavior of human proteins (14,15).

Our study results are limited in several aspects. Only one tumor type was examined in a heterotopic, subcutaneous rat model with potentially altered tumor physiology. Only one inhibitor of angiogenesis, the VEGF-antibody bevacizumab, was examined at one posttreatment time point (24 hours) and only one comparison contrast agent (albumin-[Gd-DTPA]<sub>35</sub>) was included. Earlier time points were not tested in this study, but may also have been able to show a permeability response. By necessity, the subject population was limited to animals. Pending future governmental approval of MMCM for human use, a similar study in patients could evaluate possible advantages of macromolecular MRI contrast media for monitoring antiangiogenic therapy in a clinical setting.

In conclusion, the novel macromolecular contrast agent PEG12,000-Gen4-(Gd-DOTA)<sub>16</sub>, based on PEG and developed for clinical development, was successfully applied for monitoring the early antiangiogenic effects of bevacizumab in a human melanoma model in rats using DCE-MRI. Validation experiments using the established prototype MMCM albumin-(Gd-DTPA)<sub>35</sub> revealed a comparable performance for both macromolecular compounds in the investigated experimental setup. Current study results support the hypothesis that DCE-MRI enhanced with the innovative macromolecular contrast medium PEG12,000-Gen4-(Gd-DOTA)<sub>16</sub> could be a valuable tool to individually tailor antiangiogenesis drug treatment. Similarly, the same MRI technique could help to individualize decisions on dosage and optimal timing for drug administration.

## Acknowledgments

This work was supported by National Institutes of Health grant R01 CA082923.

## References

1. Ratain MJ, Eisen T, Stadler WM, et al. Phase II placebo-controlled randomized discontinuation trial of sorafenib in patients with metastatic renal cell carcinoma. *J Clin Oncol*. 2006; 24:2505–2512. <http://dx.doi.org/10.1200/JCO.2005.03.6723>. [PubMed: 16636341]
2. Wahl RL, Jacene H, Kasamon Y, et al. From RECIST to PERCIST: evolving considerations for PET response criteria in solid tumors. *J Nucl Med*. 2009; 50(Suppl 1):122S–150S. [http://dx.doi.org/50/Suppl\\_1/122S\[pil\]10.2967/jnumed.108.057307](http://dx.doi.org/50/Suppl_1/122S[pil]10.2967/jnumed.108.057307). [PubMed: 19403881]
3. Brasch R, Pham C, Shames D, et al. Assessing tumor angiogenesis using macromolecular MR imaging contrast media. *J Magn Reson Imaging*. 1997; 7:68–74. [PubMed: 9039595]
4. Cyran CC, Sennino B, Chaopathomkul B, et al. Magnetic resonance imaging for monitoring the effects of thalidomide on experimental human breast cancers. *Eur Radiol*. 2009; 19:121–131. [PubMed: 18665367]
5. Fournier LS, Novikov V, Lucidi V, et al. MR monitoring of cyclooxygenase-2 inhibition of angiogenesis in a human breast cancer model in rats. *Radiology*. 2007; 243:105–111. [PubMed: 17329684]



6. Pham CD, Roberts TP, van Bruggen N, et al. Magnetic resonance imaging detects suppression of tumor vascular permeability after administration of antibody to vascular endothelial growth factor. *Cancer Invest.* 1998; 16:225–230. [PubMed: 9589031]
7. Grist TM, Korosec FR, Peters DC, et al. Steady-state and dynamic MR angiography with MS-325: initial experience in humans. *Radiology.* 1998; 207:539–544. [PubMed: 9577507]
8. Henderson E, Sykes J, Drost D, et al. Simultaneous MRI measurement of blood flow, blood volume, and capillary permeability in mammary tumors using two different contrast agents. *J Magn Reson Imaging.* 2000; 12:991–1003. [PubMed: 11105041]
9. Li D, Zheng J, Weinmann HJ. Contrast-enhanced MR imaging of coronary arteries: comparison of intra- and extravascular contrast agents in swine. *Radiology.* 2001; 218:670–678. [PubMed: 11230638]
10. Bumb A, Brechbiel MW, Choyke P. Macromolecular and dendrimer-based magnetic resonance contrast agents. *Acta Radiol.* 2010; 51:751–767. <http://dx.doi.org/10.3109/02841851.2010.491091>. [PubMed: 20590365]
11. Ye Z, Wu X, Tan M, et al. Synthesis and evaluation of a polydisulfide with Gd-DOTA monoamide side chains as a biodegradable macromolecular contrast agent for MR blood pool imaging. *Contrast Media Mol Imaging.* 2013; 8:220–228. <http://dx.doi.org/10.1002/cmml.1520>. [PubMed: 23606425]
12. Lim J, Turkbey B, Bernardo M, et al. Gadolinium MRI contrast agents based on triazine dendrimers: relaxivity and in vivo pharmacokinetics. *Bioconjug Chem.* 2012; 23:2291–2299. <http://dx.doi.org/10.1021/bc300461r>. [PubMed: 23035964]
13. Raatschen HJ, Fu Y, Shames DM, et al. Magnetic resonance imaging enhancement of normal tissues and tumors using macromolecular Gd-based cascade polymer contrast agents: preclinical evaluations. *Invest Radiol.* 2006; 41:860–867. [PubMed: 17099424]
14. Cyran CC, Fu Y, Raatschen HJ, et al. New macromolecular polymeric MRI contrast agents for application in the differentiation of cancer from benign soft tissues. *J Magn Reson Imaging.* 2008; 27:581–589. [PubMed: 18219614]
15. Fu Y, Raatschen HJ, Nitecki DE, et al. Cascade polymeric MRI contrast media derived from poly(ethylene glycol) cores: initial syntheses and characterizations. *Biomacromolecules.* 2007; 8:1519–1529. <http://dx.doi.org/10.1021/bm061141h>. [PubMed: 17402781]
16. Cai J, Han S, Qing R, et al. In pursuit of new anti-angiogenic therapies for cancer treatment. *Front Biosci.* 2011; 16:803–814.
17. Rose S. FDA pulls approval for avastin in breast cancer. *Cancer Discovery.* 2011; 1:OF1–OF2. <http://dx.doi.org/10.1158/2159-8290.CD-ND112311OL-08>.
18. Dienstmann R, Ades F, Saini KS, et al. Benefit-risk assessment of bevacizumab in the treatment of breast cancer. *Drug Saf.* 2012; 35:15–25. [PubMed: 22136182]
19. Shames DM, Kuwatsuru R, Vexler V, et al. Measurement of capillary permeability to macromolecules by dynamic magnetic resonance imaging: a quantitative noninvasive technique. *Magn Reson Med.* 1993; 29:616–622. [PubMed: 8505897]
20. Fu Y, Nitecki DE, Maltby D, et al. Dendritic iodinated contrast agents with PEG-cores for CT imaging: synthesis and preliminary characterization. *Bioconjug Chem.* 2006; 17:1043–1056. [PubMed: 16848414]
21. Ogan MD, Schmiedl U, Moseley ME, et al. Albumin labeled with Gd-DTPA. An intravascular contrast-enhancing agent for magnetic resonance blood pool imaging: preparation and characterization. *Invest Radiol.* 1987; 22:665–671. [PubMed: 3667174]
22. Roberts TP, Brasch RC, Schwickert HC, et al. Quantification of tissue gadolinium concentration using magnetic resonance imaging: comparison of ultrashort inversion time inversion recovery echoplanar and dynamic three-dimensional spoiled gradient-recalled approaches with in vitro measurements. *Acad Radiol.* 1996; 3(Suppl 2):S282–S285. [PubMed: 8796581]
23. Preda A, Turetschek K, Daldrup H, et al. The choice of region of interest measures in contrast-enhanced magnetic resonance image characterization of experimental breast tumors. *Invest Radiol.* 2005; 40:349–354. [PubMed: 15905721]

24. Stephen RM, Gillies RJ. Promise and progress for functional and molecular imaging of response to targeted therapies. *Pharm Res.* 2007; 24:1172–1185. <http://dx.doi.org/10.1007/s11095-007-9250-3>. [PubMed: 17385018]
25. Menichetti L, Manzoni L, Paduano L, et al. Iron oxide-gold core-shell nanoparticles as multimodal imaging contrast agent. *IEEE Sensors J.* 2013; 13:2305–2312.
26. Casciaro S, Soloperto G, Greco A, et al. Effectiveness of functionalized nanosystems for multimodal molecular sensing and imaging in medicine. *IEEE Sensors J.* 2013; 13:2305–2312.
27. Malvindi MA, Greco A, Conversano F, et al. Magnetic/silica nanocomposites as dual-mode contrast agents for combined magnetic resonance imaging and ultrasonography. *Adv Funct Mater.* 2011; 21:2548–2555.
28. Kiessling F, Farhan N, Lichy MP, et al. Dynamic contrast-enhanced magnetic resonance imaging rapidly indicates vessel regression in human squamous cell carcinomas grown in nude mice caused by VEGF receptor 2 blockade with DC101. *Neoplasia.* 2004; 6:213–223. <http://dx.doi.org/10.1593/neo.3394>. [PubMed: 15153333]
29. Turetschek K, Preda A, Novikov V, et al. Tumor microvascular changes in antiangiogenic treatment: assessment by magnetic resonance contrast media of different molecular weights. *J Magn Reson Imaging.* 2004; 20:138–144. [PubMed: 15221819]
30. Cyran CC, Paprottka PM, Schwarz B, et al. Perfusion MRI for monitoring the effect of sorafenib on experimental prostate carcinoma: a validation study. *AJR Am J Roentgenol.* 2012; 198:384–391. <http://dx.doi.org/10.2214/AJR.11.6951>. [PubMed: 22268182]
31. Afaq A, Akin O. Imaging assessment of tumor response: past, present and future. *Future Oncol.* 2011; 7:669–677. [PubMed: 21568682]
32. Cyran CC, Sennino B, Fu Y, et al. Permeability to macromolecular contrast media quantified by dynamic MRI correlates with tumor tissue assays of vascular endothelial growth factor (VEGF). *Eur J Radiol.* 2012; 81:891–896. <http://dx.doi.org/10.1016/j.ejrad.2011.07.016>. [PubMed: 21889860]
33. Dvorak HF, Sioussat TM, Brown LF, et al. Distribution of vascular permeability factor (vascular endothelial growth factor) in tumors: concentration in tumor blood vessels. *J Exp Med.* 1991; 174:1275–1278. [PubMed: 1940805]

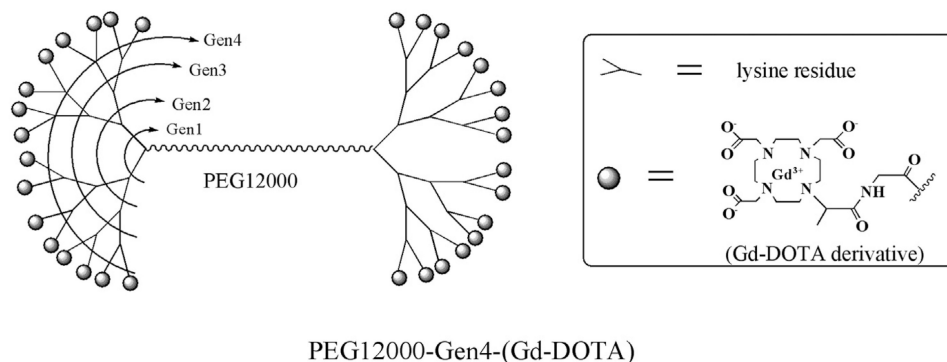


**Figure 1.** Schematic chemical structure of the polyethylene glycol (PEG) core dendrimeric contrast agent PEG12,000-Gen4-(Gd-DOTA)<sub>16</sub>. This new class of macromolecular contrast medium consists of a linear PEG core and two peripheral lysine-dendrimer amplifiers, which are conjugated, with multiple highly stable Gd-DOTA chelates serving as signal enhancing groups in magnetic resonance imaging. PEG12,000-Gen4-(Gd-DOTA)<sub>16</sub>, being extremely hydrophilic and bulky, creates a water shield around the polymer, making the effective size (molecular weight [MW] = 194 kDa) much greater than indicated by the actual MW (27 kDa).

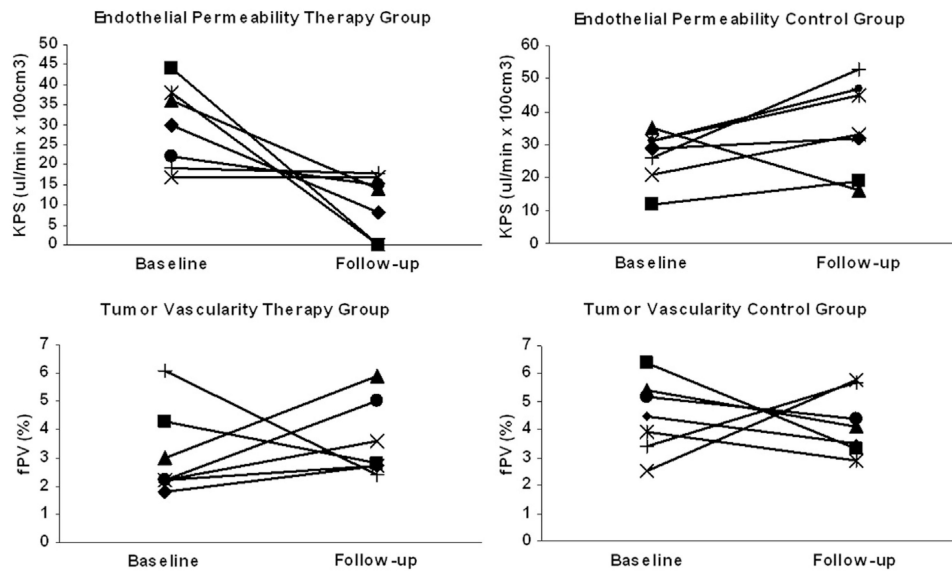


**Figure 2.**

Line graphs depict the development of individual values for polyethylene glycol 12,000-Gen4-(Gd-DOTA)<sub>16</sub> for tumor endothelial permeability and tumor vascularity from baseline to follow-up (24 hours) in the therapy and the control groups. Note the decline of endothelial-surface permeability constant ( $K^{PS}$ ) after a single intraperitoneal dose of 1 mg bevacizumab in the therapy group as well as the omnidirectional development of  $K^{PS}$  in the control group. No significant effects on tumor vascularity were noted in the therapy or in the control groups.

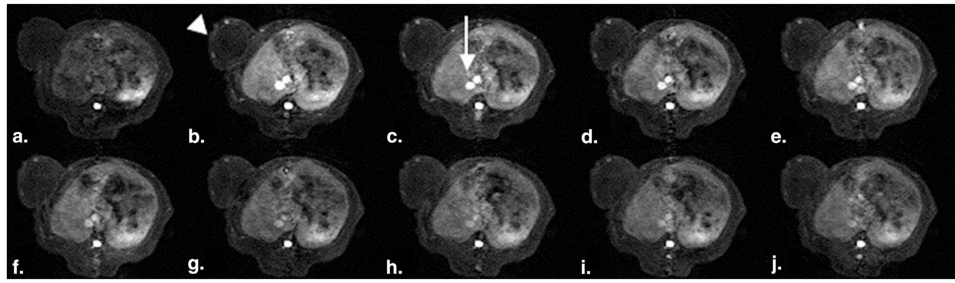


**Figure 3.** (a-j). Representative set of T1-weighted spoiled gradient dynamic magnetic resonance images enhanced with the candidate polymer macromolecular contrast medium polyethylene glycol 12,000-Gen4-(Gd-DOTA)<sub>16</sub> precontrast and 2, 5, 10, 15, 20, 25, 30, 40, 50, and 60 minutes after injection. Note the enhancement of the human cancer xenograft over the left lateral flank (*arrowhead*), most prominent in the tumor periphery, as well as the strong and time persistent enhancement of the inferior vena cava (*arrow*) as it passes through the rat liver.

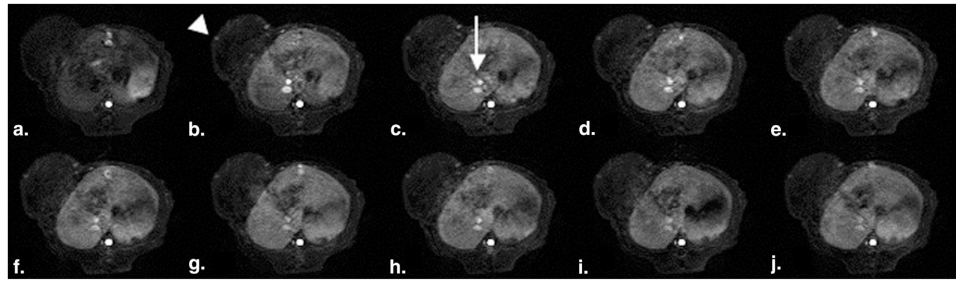


**Figure 4.** (a-j). Representative set of T1-weighted spoiled gradient dynamic magnetic resonance images enhanced with the prototype macromolecular contrast medium albumin-(Gd-DTPA)<sub>35</sub> precontrast and 2, 5, 10, 15, 20, 25, 30, 40, 50, and 60 minutes after injection. Note the enhancement of the human cancer xenograft over the left lateral flank (*arrowhead*), most prominent in the tumor periphery, as well as the strong and time persistent enhancement of the inferior vena cava (*arrow*) as it passes through the rat liver.



**Table 1**  
**Individual Values of K<sup>PS</sup> and fPV Quantified by DCE-MRI Enhanced With the Polymer MMCM PEG12,000-Gen4-(Gd-DOTA)<sub>16</sub> and the MMCM Prototype Albumin-(Gd-DTPA)<sub>35</sub> at Baseline and 24 Hours After a Single Intraperitoneal Injection of the Monoclonal Anti-VEGF Antibody Bevacizumab**

Tumor	Therapy				Control			
	Baseline		Follow-up		Baseline		Follow-up	
	K <sup>PS</sup> (μL·min·100 cm <sup>3</sup> )	fPV (%)	K <sup>PS</sup> (μL·min·100 cm <sup>3</sup> )	fPV (%)	K <sup>PS</sup> (μL·min·100 cm <sup>3</sup> )	fPV (%)	K <sup>PS</sup> (μL·min·100 cm <sup>3</sup> )	fPV (%)
1	30	1.8	8	2.7	29	4.5	32	3.5
2	44	4.3	0	2.8	118	6.4	19	3.3
3	36	3.0	14	5.9	35	5.4	15	4.1
4	17	2.2	17	3.6	21	2.5	33	5.8
5	38	2.2	0	2.7	31	3.9	45	2.9
6	22	2.2	15	5.0	31	5.1	47	4.4
7	19	6.1	18	2.4	26	3.4	53	5.7
Mean ± SD	29.5 ± 10.4	3.1 ± 1.6	10.4 ± 7.8*	3.6 ± 1.4	41 ± 34	4.5 ± 1.3	35 ± 14	4.2 ± 1.1
	Therapy				Control			
	Baseline		Follow-up		Baseline		Follow-up	
	K <sup>PS</sup> (μL·min·100 cm <sup>3</sup> )	fPV (%)	K <sup>PS</sup> (μL·min·100 cm <sup>3</sup> )	fPV (%)	K <sup>PS</sup> (μL·min·100 cm <sup>3</sup> )	fPV (%)	K <sup>PS</sup> (μL·min·100 cm <sup>3</sup> )	fPV (%)
1	11	3.3	0	2.8	16	2.6	7	2.7
2	45	5.2	0	2.6	34	4.1	10	2.4
3	16	2.8	0	3.3	27	3.3	15	4.3
4	45	6.2	0	6.5	37	3.7	12	1.8
5	35	4.6	0	8.4	38	3.5	19	3.0
6	38	5.6	0	3.7	13	1.9	11	1.1
Mean ± SD	32 ± 15	4.6 ± 1.3	0*	4.5 ± 2.3	28 ± 11	3.2 ± 0.8	12 ± 4	2.5 ± 1

DCE, dynamic contrast-enhanced; fPV, tumor vascularity; K<sup>PS</sup>, tumor endothelial permeability; MMCM, macromolecular contrast medium; MRI, magnetic resonance imaging; PEG, poly ethylene; SD, standard deviation; VEGF, vascular endothelial growth factor.

\* Significantly different to baseline.

**Table 2**  
**Theoretical and Measured Effective MW, T1 Relaxivities, and Blood Half-Lives for PEG12,000-Gen4-(Gd-DOTA) and Albumin-(Gd-DTPA)<sub>35</sub>**

Contrast Agent	Theoretical MW (kDa)	Effective MW (kDa)	T1 Relaxivity per Gd Ion (mM <sup>-1</sup> ·s <sup>-1</sup> )	Blood Half-Life Mean ± SD (Minutes)
PEG12,000-Gen4-(Gd-DOTA) <sub>16</sub>	27	194	9.9	49 ± 6
Albumin-(Gd-DTPA) <sub>35</sub>	92	180	10.4	54 ± 11

MW, molecular weight; PEG, polyethylene glycol; SD, standard deviation.

Effective molecular weights were determined by comparison to protein standards on size exclusion chromatography. T1 relaxivities were measured at 10 MHz and 37°C.